Regulation of photoprotection gene expression in *Chlamydomonas* by a putative E3 ubiquitin ligase complex and a homolog of CONSTANS

Stéphane T. Gabilly[a,1], Christopher R. Baker[a,b,1], Setsuko Wakao[a,c,1], Thien Crisanto[a], Katharine Guan[a,b], Ke Bi[d], Elodie Guiet[a], Carmela R. Guadagno[a,2], and Krishna K. Niyogi[a,b,c,3]

[a]Department of Plant and Microbial Biology, University of California, Berkeley, CA 94720; [b]Howard Hughes Medical Institute, University of California, Berkeley, CA 94720; [c]Molecular Biophysics and Integrated Bioimaging Division, Lawrence Berkeley National Laboratory, Berkeley, CA 94720; and [d]Computational Genomics Resource Laboratory, California Institute for Quantitative Biosciences, University of California, Berkeley, CA 94720

Photosynthetic organisms use nonphotochemical quenching (NPQ) mechanisms to dissipate excess absorbed light energy and protect themselves from photooxidation. In the model green alga *Chlamydomonas reinhardtii*, the capacity for rapidly reversible NPQ (qE) is induced by high light, blue light, and UV light via increased expression of *LHCSR* and *PSBS* genes that are necessary for qE. Here, we used a forward genetics approach to identify SPA1 and CUL4, components of a putative green algal E3 ubiquitin ligase complex, as critical factors in a signaling pathway that controls light-regulated expression of the *LHCSR* and *PSBS* genes in *C. reinhardtii*. The *spa1* and *cul4* mutants accumulate increased levels of LHCSR1 and PSBS proteins in high light, and unlike the wild type, they express LHCSR1 and exhibit qE capacity even when grown in low light. The *spa1-1* mutation resulted in constitutively high expression of *LHCSR* and *PSBS* RNAs in both low light and high light. The qE and gene expression phenotypes of *spa1-1* are blocked by mutation of CrCO, a B-box Zn-finger transcription factor that is a homolog of CONSTANS, which controls flowering time in plants. CONSTANS-like *cis*-regulatory sequences were identified proximal to the qE genes, consistent with CrCO acting as a direct activator of qE gene expression. We conclude that SPA1 and CUL4 are components of a conserved E3 ubiquitin ligase that acts upstream of CrCO, whose regulatory function is wired differently in *C. reinhardtii* to control qE capacity via *cis*-regulatory CrCO-binding sites at key photoprotection genes.

light harvesting | light signaling | nonphotochemical quenching | photomorphogenesis | photosynthesis

Light is necessary for photosynthesis, but the supply of light in natural environments is not constant. Photosynthetic organisms have evolved functional flexibility in their light-harvesting systems, enabling efficient absorption and utilization of limiting light and photoprotection in excess light. In saturating light, photosynthetic light harvesting is regulated by nonphotochemical quenching (NPQ) mechanisms that are responsible for dissipating excess absorbed light energy as heat (1, 2).

NPQ involves the deexcitation of singlet excited chlorophyll (^{1}Chl*) in photosystem II (PSII), and the term NPQ reflects the way in which these processes are routinely assayed through measurements of chlorophyll fluorescence quenching (3). The major component of NPQ under most short-term light stress conditions is called qE (1, 2, 4). It is turned on and off rapidly (seconds to minutes) and depends on the formation of a large ΔpH across the thylakoid membrane in excess light (5). In the reference green alga *Chlamydomonas reinhardtii*, a light-harvesting complex (LHC) protein called LHCSR functions as both a sensor of lumen pH and a site of qE to which pigments are bound (6–9). *C. reinhardtii* has 3 genes encoding LHCSR: *LHCSR1*, *LHCSR3.1*, and *LHCSR3.2* (6). In plants, another member of the LHC protein superfamily, PSBS, is a major sensor of lumen pH (10) that turns qE on and off by somehow facilitating a rearrangement of LHC proteins that surround PSII (11–15). PSBS also appears to

contribute to qE in *C. reinhardtii* (16–18), which has 2 closely linked *PSBS* genes, *PSBS1* and *PSBS2* (19).

LHCSR expression and qE capacity in *C. reinhardtii* are inducible by exposure to high light (6), UV light (18), and blue light (20), whereas cells grown in low light have a very limited qE capacity (6). Induction of LHCSR expression and qE involves photoreceptors such as UVR8 (18, 21) and phototropin (PHOT) (20), however the signaling components that act downstream of the photoreceptors to regulate LHCSR expression have not been elucidated (22). Here, we describe the results of a genetic screen in which we isolated mutants that overexpress LHCSR1 and PSBS. These mutants have an increased capacity for qE even when grown in low light, and they show that a conserved E3 ubiquitin ligase complex (23–25) is involved in the regulation of *LHCSR* and *PSBS* gene expression via an ortholog of the plant transcription factor CONSTANS (26).

Results

Identification and Genetic Analysis of Suppressors of *npq4*. We performed a suppressor screen designed to isolate mutants that

---

Significance

Photoprotection is an indispensable component of abiotic stress tolerance in all photosynthetic organisms. In contrast to land plants, the transcript abundance of photoprotection genes is strongly controlled by light in the model green alga *Chlamydomonas reinhardtii*. Here we show that the repression of photoprotection genes in low light depends on 2 putative components of a conserved E3 ubiquitin ligase complex. We also show that this regulation of gene expression depends on a transcription factor that is conserved among plants and algae and that acts downstream of the putative E3 ubiquitin ligase complex. Our work provides mechanistic insight into how a deeply conserved light signaling pathway is wired differently in *C. reinhardtii*, giving rise to light control of photoprotection gene expression.

---

overaccumulate LHCSR1 and/or PSBS by UV mutagenizing the *C. reinhardtii npq4* mutant and screening for colonies with increased NPQ using video imaging of chlorophyll fluorescence (27). The *npq4* mutant exhibits low qE capacity, because it lacks functional *LHCSR3.1* and *LHCSR3.2* genes (6), but it retains intact copies of *LHCSR1*, *PSBS1*, and *PSBS2*. Therefore, we hypothesized that overexpression of one or more of these genes would be a simple mechanism for increasing qE in *npq4*. Among ~10,000 mutagenized colonies, 30 mutants showed reproducibly elevated NPQ values relative to the *npq4* parent strain. Fig. 1 shows the kinetics of NPQ induction and relaxation for 3 *npq4* suppressors (*spa1-1*, *spa1-2*, and *cul4-1*) that we selected for further analysis. These suppressors showed NPQ levels that were intermediate between the *npq4* parent and the wild-type (WT) strain after growth in high light (HL) (Fig. 1*B*), and they also displayed higher NPQ relative to *npq4* and the WT strain after growth in the noninducing condition of low light (LL) (Fig. 1*A*). The NPQ observed in these 3 suppressors was rapidly reversible in the dark (Fig. 1), indicating that the qE component of NPQ was increased.

To determine if the *npq4* suppressors overaccumulate LHCSR1 and/or PSBS, we examined levels of these proteins by immunoblot analysis of LL- and HL-grown cells. In WT, LHCSR protein was only detected in HL-grown cells (*SI Appendix*, Fig. S1). In contrast, the *npq4* suppressors accumulated high levels of LHCSR1 in both inducing (HL) and noninducing conditions (LL), and the LHCSR1 levels in HL were elevated relative to those observed in *npq4*. We were also able to detect PSBS in the 3 *npq4* suppressors when grown in HL (*SI Appendix*, Fig. S1). This was an unanticipated result given that detection of PSBS in *C. reinhardtii* has previously been observed only transiently in stress conditions such as during the first hours of exposure to very high light (16), damaging levels of UV-B radiation (18), or HL in combination with low CO_2 (17).

Backcrossing the 3 *npq4* suppressors to *npq4* revealed a 2:2 segregation of the NPQ phenotype (*SI Appendix*, Fig. S2), showing that the high NPQ phenotype is the result of a single nuclear mutation in each case. We segregated the suppressor mutation in each of these 3 lines from the *npq4* mutation by crossing to WT. Analysis of progeny of tetratype tetrads showed that the high NPQ phenotype of the suppressor mutations in LL- and HL-grown cells was also evident in a WT background (*SI Appendix*, Fig. S3).

Molecular Analysis of *spa1* and *cul4* Mutations. The causative suppressor mutations were identified by a combination of whole-genome sequencing and bulked segregant analysis of backcross progeny (Fig. 2*A*). Briefly, the NPQ values of backcross progeny were quantified (*SI Appendix*, Fig. S2), and pools of low and high

NPQ progeny were constructed and sequenced, along with the parents. In both *spa1-1* and *spa1-2*, the putative causative polymorphisms were mapped to independent missense mutations at conserved residues in Cre13.g602700, an ortholog of *Arabidopsis thaliana SPA1* (Fig. 2*B* and *SI Appendix*, Fig. S4 and Table S1). The putative causative polymorphism in *cul4-1* was identified as a missense mutation at a conserved residue in Cre12.g516500, an ortholog of *A. thaliana CUL4* (Fig. 2*C* and *SI Appendix*, Fig. S4 and Table S2). We confirmed that expression of a wild-type version of *SPA1* rescued the NPQ phenotype of *npq4 spa1-1* (*SI Appendix*, Fig. S5). Of the 3 suppressors, *spa1-1* was selected for complementation and further analysis, because it exhibited the strongest induction of NPQ in LL (*SI Appendix*, Fig. S3).

In *A. thaliana*, both SPA1 and CUL4 are subunits of the COP1-SPA E3 ubiquitin ligase complex (28) that is involved in light signaling and photomorphogenesis (23–25). SPA1-SPA4 and COP1 are paralogous WD40 repeat domain-containing proteins, and 2 copies of SPA and 2 copies of COP1 form a heterotetramer (29), which acts as the substrate acceptor domain of the E3 ubiquitin ligase complex (28). Unlike COP1, SPA proteins contain a Ser/Thr kinase-like domain (Fig. 2*B*), which has been shown to have a regulatory role in modulating the activity of the complex (30, 31). In *C. reinhardtii*, which has a single *SPA* gene, the *spa1-1* mutation maps to the Ser/Thr kinase-like domain (*SI Appendix*, Fig. S4*A*), whereas *spa1-2* maps to the WD40 repeat domain (*SI Appendix*, Fig. S4*B*). Notably, missense mutations in the Ser/Thr kinase-like domain of *SPA1* in *A. thaliana* induced a loss-of-function phenotype (30). CUL4 acts as a scaffold protein within *A. thaliana* CUL4-DDB1 E3 ubiquitin ligase complexes, connecting the COP1-SPA substrate acceptor domain to the E3 ubiquitin ligase (28). CUL4 contains both Cullin and winged helix protein interaction domains (Fig. 2*C*), and the *cul4-1* mutation in *C. reinhardtii* maps to the Cullin domain (*SI Appendix*, Fig. S4*C*).

The *C. reinhardtii* Homolog of CONSTANS Acts Downstream of SPA1. Using de novo motif identification software (32), we identified a promoter sequence, shared within ~350 bp of the translation start site of all 5 of the qE genes (*LHCSR1*, *LHCSR3.1*, *LHCSR3.2*, *PSBS1*, and *PSBS2*) in *C. reinhardtii* (Fig. 3). This motif with a CCACA core strongly resembles the binding site for the plant transcription factor CONSTANS (CO) (33), a well-known substrate protein that COP1-SPA targets to the E3 ubiquitin ligase complex in *A. thaliana* (34–36). *C. reinhardtii* has a homolog of CO, called CrCO, with a conserved function in circadian gene regulation and a conserved DNA-binding specificity as demonstrated by complementation of the *A. thaliana co* mutant by CrCO (26). We previously identified a mutant (CAL028_01_08) affected in CrCO
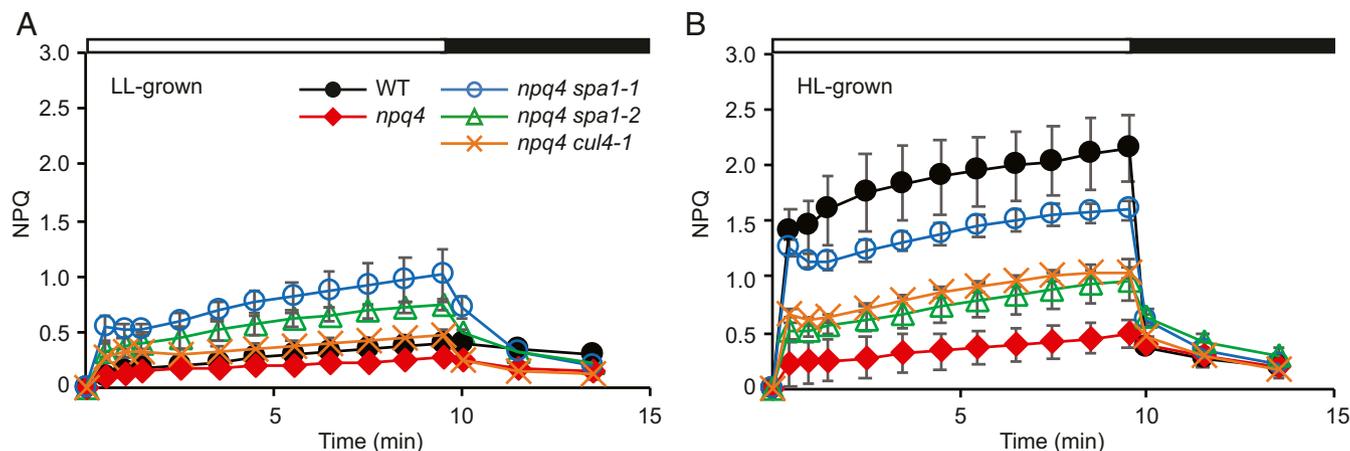
Fig. 1. Three suppressors of *npq4* have elevated NPQ capacity when grown in LL (60 μmol photons $m^{-2} s^{-1}$) or HL (350 μmol photons $m^{-2} s^{-1}$). NPQ was induced with actinic light of 600 μmol photons $m^{-2} s^{-1}$ (white bar at *Top*), followed by recovery in the dark with 0.6 μmol photons $m^{-2} s^{-1}$ far-red light (black bar at *Top*). (*A*) LL-grown cells. (*B*) Cells grown in HL for 3 d. Values represent means ± SD (n = 3).

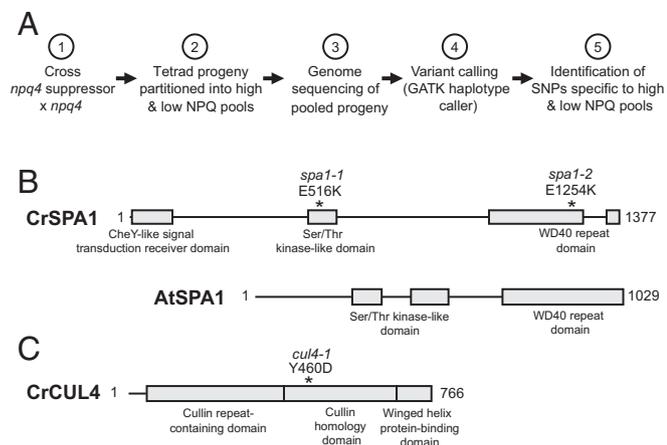**Fig. 2.** Identification of causative polymorphisms in suppressor mutants. (*A*) General outline of workflow for bulked segregant analysis and genome sequencing to identify causative SNPs in UV-mutagenized *npq4* suppressors. (*B*) Protein domain predictions for CrSPA1 and AtSPA1 and (*C*) CrCUL4, with locations of suppressor mutations (*spa1-1*, *spa1-2*, and *cul4-1*) marked by asterisks.

(Cre06.g278159) in our collection of DNA insertional mutants (37). Analysis of PCR products across the gene showed that the mutant has a deletion affecting the *CrCO* gene, whereas the flanking genes were intact (*SI Appendix*, Fig. S6 *A* and *B*). The *crco* mutant exhibited a severe defect in NPQ, specifically qE (Fig. 4), that cosegregated 2:2 with the paromomycin resistance cassette used for insertional mutagenesis (*SI Appendix*, Fig. S6C), and the mutant was sensitive to HL (*SI Appendix*, Fig. S7). Additionally, the low NPQ phenotype of the *crco* mutant could be rescued by complementation with a wild-type version of *CrCO* (*SI Appendix*, Fig. S6D), confirming that the phenotype is caused by the *crco* deletion.

To determine if CrCO is a downstream target of the putative COP1-SPA1 E3 ubiquitin ligase complex in *C. reinhardtii*, *crco* was crossed with *spa1-1* to generate a *crco spa1-1* double mutant. The double mutant had the same low NPQ phenotype as the *crco* single mutant (Fig. 4 *A* and *B*), implying that SPA1 and CrCO act in the same pathway with CrCO downstream of SPA1. Because *A. thaliana* CO is a transcriptional regulator, we next examined whether transcript levels of the genes necessary for qE were affected in these mutants. Specifically, we measured transcript abundance for *LHCSR1*, *LHCSR3.1*, *LHCSR3.2*, *PSBS1*, and *PSBS2* in 4 genotypes: WT, *spa1-1*, *crco*, and *crco spa1-1*. In *spa1-1*, each qE gene was expressed in LL at levels comparable to WT in HL (Fig. 4C), showing that *spa1-1* disrupts the normal light-dependent expression of qE genes at the RNA level. The *crco* and *crco spa1-1* mutants showed severely diminished expression of all 5 qE genes in both LL and HL, although some degree of HL induction persists (Fig. 4C). In fact, for *LHCSR3.1* and *LHCSR3.2*, while *crco* and *crco spa1-1* share the same diminished transcript abundance relative to WT for all 5 qE genes, the HL-induced fold induction at specifically these 2 genes remains robust.

At the protein level, the overaccumulation of LHCSR1 and PSBS observed in *spa1-1* in HL (Fig. 4 *C* and *D* and *SI Appendix*, Fig. S1) is correlated with their elevated transcript abundance. Similarly, the elevated transcript level of *LHCSR1* in LL is associated with high LHCSR1 protein levels in LL (Fig. 4 *C* and *D*); however, this was not the case for either LHCSR3 or PSBS in LL. LHCSR3 in LL-grown *spa1-1* was detected at a similar level to WT LL (Fig. 4D), despite a large overaccumulation of *LHCSR3.1* and *LHCSR3.2* transcripts in *spa1-1* LL (Fig. 4C). A similar trend emerged for PSBS. We observed a high accumulation of PSBS in *spa1-1* HL and a relatively low level in WT HL. However, the levels of *PSBS1* and *PSBS2* transcripts in *spa1-1* LL were equal to or greater than, respectively, their levels in WT HL, and yet we were unable to detect PSBS protein in *spa1-1* LL. These results

support the existence of a SPA1-independent, posttranscriptional regulatory mechanism that controls protein levels of LHCSR3 and PSBS, but not LHCSR1, in a light-dependent manner.

Discussion

In this work, we demonstrate that SPA1 and CUL4, subunits of the deeply conserved COP1-SPA1 E3 ubiquitin ligase complex, are necessary for the repression of qE capacity in LL-grown *C. reinhardtii* (Fig. 5). Furthermore, we show that CrCO, an ortholog of the *A. thaliana* CO transcription factor, is necessary for the expression of *LHCSR* and *PSBS* genes and that it is downstream of SPA1-mediated control of qE gene expression and qE capacity. By analogy with *A. thaliana*, our data strongly indicate that the COP1-SPA1 complex serves as a substrate receptor for a CUL4-DDB1 E3 ligase (28) to control degradation of CrCO in response to light signals in *C. reinhardtii* (Fig. 5). However, in contrast to *A. thaliana*, the target genes of CrCO are wired differently with CO-like binding sites in the promoter sequences for qE genes, thus ultimately placing photoprotection under the control of COP1-SPA1 E3 ubiquitin ligase-mediated signaling in *C. reinhardtii*. Based on analysis of promoters (Fig. 3) and transcript levels (Fig. 4C), we suggest that CrCO regulates qE gene transcription through direct promoter binding (Fig. 5). We also find evidence that there is at least 1 other pathway that operates independently of SPA1 and CrCO to control the HL induction of gene expression for these qE genes (Figs. 4 and 5). Finally, our work also highlights that there are mechanisms beyond transcriptional control that are necessary to explain the complexity of protein abundance for LHCSR3 and PSBS.

It was recently reported that another E3 ubiquitin ligase complex is involved in regulating LHCSR1 and LHCSR3 expression in *C. reinhardtii* (38). In this work, mutations in *DET1* and *DDB1*, which encode 2 subunits of a putative CUL4-DDB1^DET1 E3 ligase complex, were shown to lead to accumulation of *LHCSR1*, *LHCSR3*, and *PSBS* transcripts in the dark, similar to what we observed in LL. In *A. thaliana*, DET1 E3 ligase complexes are distinct in composition from the COP1-SPA1 complex, although CUL4 and DDB1 are subunits of both types of complexes (39). We propose 2 plausible models to synthesize our results with those found for the DET1 complex. In 1 model, the DET1 and the COP1-SPA1 E3 ubiquitin ligase complexes are both necessary to
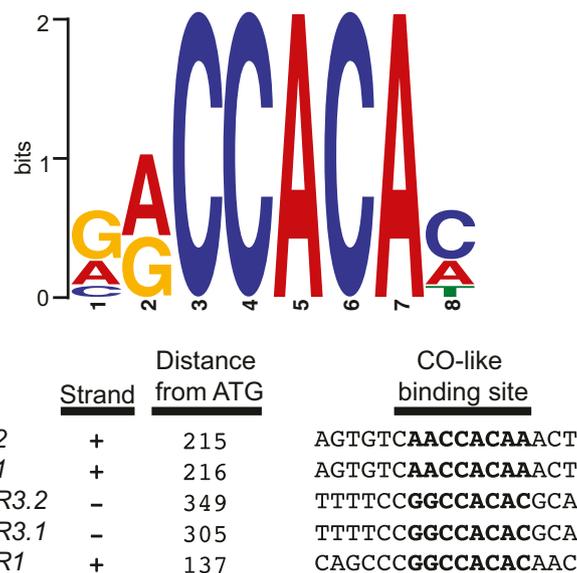

Fig. 3. Identification of CO-like *cis*-regulatory binding sites upstream of qE genes. Position-specific weight matrix generated de novo for the CO-like binding site identified upstream of the translation start site (ATG) of the *LHCSR* and *PSBS* genes. Only the single, statistically strongest matching site for each qE gene is shown in the alignment.

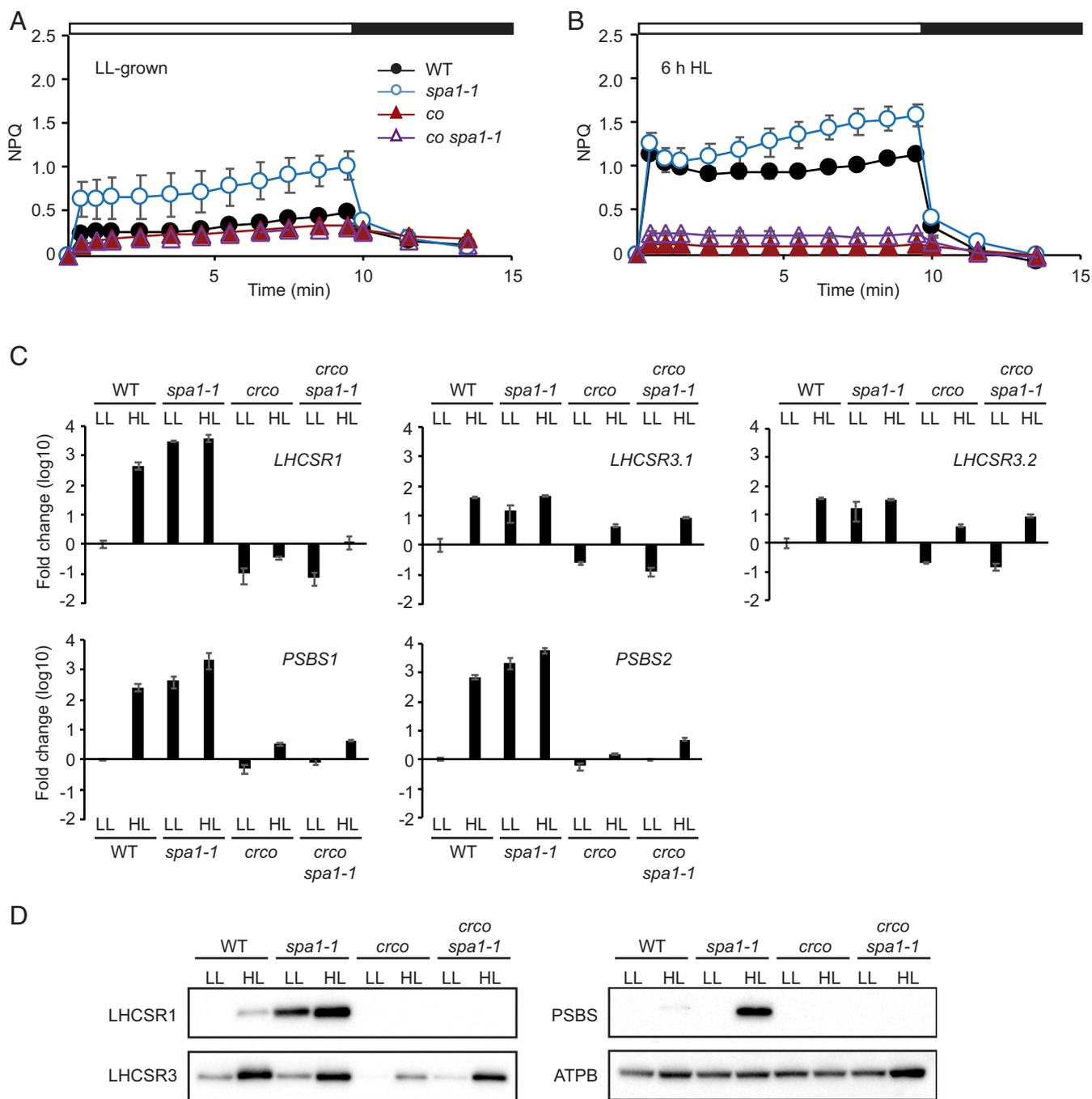|	Strand	Distance from ATG	CO-like binding site
PSBS2	+	215	AGTGTC**AACCACAA**ACT
PSBS1	+	216	AGTGTC**AACCACAA**ACT
LHCSR3.2	−	349	TTTTCC**GGCCACAC**GCA
LHCSR3.1	−	305	TTTTCC**GGCCACAC**GCA
LHCSR1	+	137	CAGCCC**GGCCACAC**AAC

Fig. 4. Deletion of *CrCO* results in low NPQ capacity, affects expression of qE genes, and blocks the high NPQ phenotype of *spa1-1* in LL. Cultures of WT, *spa1-1*, *crco*, and *crco spa1-1* were grown in LL (60 μmol photons m^{-2} s^{-1}) and exposed to HL (350 μmol photons m^{-2} s^{-1}) for 6 h to minimize photoinhibition in the *crco* strains (*SI Appendix*, Fig. S7). (*A*) NPQ of LL-grown cells. (*B*) NPQ of cells exposed to HL for 6 h. Values in *A* and *B* represent means ± SD (*n* = 3). NPQ was induced with actinic light of 600 μmol photons m^{-2} s^{-1} (white bar at *Top*), followed by recovery in the dark with 0.6 μmol photons m^{-2} s^{-1} far-red light (black bar at *Top*). (*C*) RT-qPCR analysis of RNA expression levels of *LHCSR1*, *LHCSR3.1*, *LHCSR3.2*, *PSBS1*, and *PSBS2* genes. Fold-change values for each RNA were normalized to the expression level in WT LL for that gene. CβLP was used as the internal reference. Values represent means ± SD (*n* = 3). (*D*) Immunoblot analysis of protein levels of LHCSR1, LHCSR3, and PSBS. Chloroplast ATP synthase beta-subunit (ATPB) was used as a loading control.

target CrCO for proteolysis in LL, and the loss of either complex is sufficient to allow accumulation of CrCO protein. Alternatively, the DET1 complex and the COP1-SPA1 complex may target different transcription factors, and the aberrant accumulation of either transcription factor licenses expression of the qE genes. These models are not mutually exclusive, and because *det1* mutants appear to have entirely lost light-intensity-dependent control of qE gene expression (38), DET1 might participate in multiple

pathways governing photoprotection genes, perhaps including both the SPA1/CrCO-dependent and -independent pathways depicted in Fig. 5.

Our work has directly focused on the downstream components of this signaling cascade and thus, it is interesting to speculate on what might be upstream of SPA1 in mediating light regulation of the qE genes. In plants, COP1-SPA functions in phytochrome-mediated light signaling (40, 41); however in *C. reinhardtii*,

Fig. 5. Model depicting how the COP1-SPA1 E3 ubiquitin ligase complex in *C. reinhardtii* controls the light regulation of qE gene expression through the transcriptional regulator CrCO. In low light, ubiquitination of CrCO by the COP1-SPA1 E3 ubiquitin ligase targets CrCO for degradation. The low level of CrCO that persists in low light activates low levels of transcription from the qE genes (*LHCSR1*, *LHCSR3.1*, *LHCSR3.2*, *PSBS1*, and *PSBS2*). In high light, a photoreceptor-mediated signal inhibits the COP1-SPA1 E3 ubiquitin ligase by an undefined mechanism, allowing accumulation of CrCO and its binding to the CO-like binding motif and transcriptional activation of the qE gene promoters. In addition, to explain the high-light induction of qE gene expression in the *crco* and *crco spa1-1* mutants (Fig. 4 C and D) we hypothesize the existence of a second transcriptional regulator bound to the qE gene promoters that mediates a SPA1/CrCO-independent but high-light-dependent regulatory pathway. Whether this pathway constitutes a second photoreceptor-mediated pathway, possibly integrated with a chloroplast retrograde signaling pathway, is unknown.
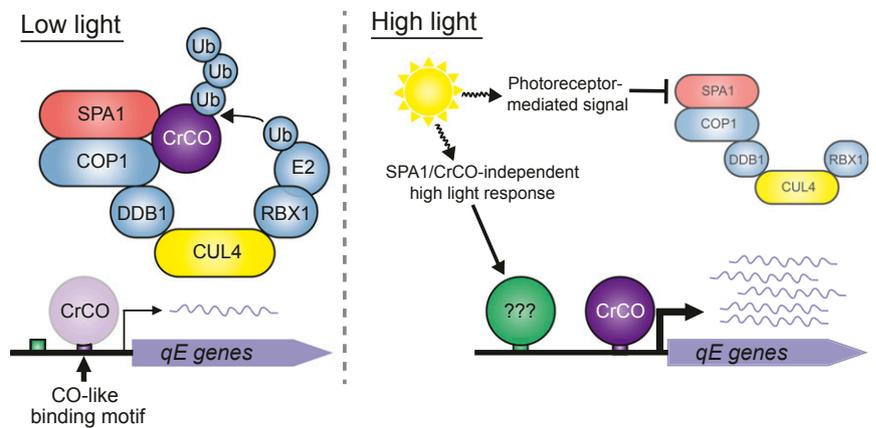
phytochrome proteins are absent (19). Thus, it seems likely that in combination with the different downstream wiring of CrCO target genes in *C. reinhardtii*, the upstream control of the COP1-SPA1 E3 ubiquitin ligase complex has also diverged. One candidate for an upstream photoreceptor controlling COP1-SPA1 activity in *C. reinhardtii* is the UV-B photoreceptor UVR8, which is known to control LHCSR1 and PSBS accumulation in *Chlamydomonas* (18, 21). In *A. thaliana*, UVR8 signaling converts COP1 from a repressor of photomorphogenesis into an activator through direct interaction with COP1 (42). It is conceivable that in *spa1-1*, mutation of a major COP1-interacting partner facilitates the interaction of UVR8 and COP1; however, UVR8 signaling in *A. thaliana* is not affected by loss of SPA proteins (43). *C. reinhardtii* also contains both plant- and animal-type cryptochromes, and cryptochromes are known to interact with SPA proteins in *A. thaliana* (44–46). A *C. reinhardtii* insertional mutant that is defective in the animal-type cryptochrome exhibits altered light-dependent expression of several genes, including *CrCO* (47), and a mutant that diminishes abundance of the plant-type cryptochrome was shown to have impaired circadian clock control (48). However, HL induction of qE capacity and LHCSR3 accumulation is unaffected in the mutant affecting the animal-type cryptochrome (20). In contrast, the importance of PHOT in the control of photoprotection in *C. reinhardtii* has been clearly established through analysis of a *phot* mutant (20). We note that the phenotypes of the *phot* and *crco* mutants are similar, which suggests that PHOT and CrCO might act in the same pathway. In the *phot* mutant, as in *crco* (Fig. 4C), *LHCSR1*, *LHCSR3.1*, *LHCSR3.2*, *PSBS1*, and *PSBS2* transcript levels are only a fraction of WT levels in HL, and yet some degree of HL induction of gene expression persists at these genes (20, 38). Induction of qE gene expression by the PHOT pathway, however, also depends on a chloroplast-derived HL signal (20), unlike the SPA1/CrCO-dependent pathway. It is possible that PHOT acts as a photoreceptor in the SPA1/CrCO-independent pathway shown in Fig. 5.

In addition, it has not escaped our notice that the chlorophyte SPA1 has a canonical CheY-like response regulator domain at its N terminus (Fig. 2B), which is absent in plant orthologs of SPA1, suggesting that a sensor histidine kinase may regulate SPA1 activity in *C. reinhardtii*. The presence of this response regulator domain in *C. reinhardtii* SPA1 might provide a clue about how the upstream regulation of the SPA1-COP1 E3 ubiquitin ligase complex has diverged from that described in *A. thaliana*. Although we have not yet characterized any point mutations in the response regulator domain of SPA1, dozens of suppressor mutants obtained in our UV mutagenesis of *npq4* remain to be sequenced.

Materials and Methods

Strains, Growth Conditions, and UV Mutagenesis. *C. reinhardtii* wild-type strain 4A+ (*mt+*, 137c background; CC-4051), *npq4* mutant defective in

LHCSR3.1 and *LHCSR3.2* genes (6), *crco* (CAL028_01_08) insertional mutant (37), and *npq4* suppressor mutants were grown in minimal high-salt medium (49) in continuous light at 60 μmol photons m^{-2} s^{-1} (LL) and 25 °C for 3 d to a cell density of 3 to 4×10^6 cells mL^{-1}, and then cells were either maintained at the same light intensity or transferred to 350 μmol photons m^{-2} s^{-1} (HL) for the specified time before harvesting cells for various measurements. Unless otherwise specified, 3 biological replicates were used. The *spa1* and *cul4* mutants were generated by UV mutagenesis of *npq4* with 6 or 7×10^4 μJ cm^{-2} of UV light (Stratalinker; Stratagene, La Jolla, CA) as previously described (50).

Chlorophyll Fluorescence Measurements. Chlorophyll fluorescence was measured at room temperature using a pulse-amplitude-modulated fluorometer (FMS2; Hansatech Instruments) or an Imaging-PAM Maxi (Walz). Cells were dark acclimated for 30 min prior to measurement, unless stated otherwise. Maximum fluorescence levels after dark acclimation (F$_m$) and maximum fluorescence levels in the light (F$_m$') were recorded after applying a saturating pulse of light. NPQ was calculated as (F$_m$ − F$_m$')/F$_m$'. For the FMS2 measurements, 3 to 5×10^7 cells were filtered onto a glass-fiber filter that was placed in the instrument's leaf clip. This was followed by an additional 5-min dark phase with far-red light of 0.6 μmol photons m^{-2} s^{-1}. F$_m$ and F$_m$' were recorded after applying a saturating pulse of 1,800 μmol photons m^{-2} s^{-1}. NPQ was induced for 9.5 min with 600 μmol photons m^{-2} s^{-1}, followed by recovery in the dark with far-red light. On the Imaging-PAM, NPQ was induced for 6 to 10 min with 550 μmol photons m^{-2} s^{-1} and relaxed for 2.5 to 8 min in the dark. False-colored NPQ images were generated by the Walz software.

Bulked Segregant Analysis and Genome Sequencing. Genetic crosses and tetrad analysis were performed according to established methods (49). The *npq4* suppressors were backcrossed to an *npq4* strain of opposite mating type. Tetrads were dissected, and the NPQ phenotype of all progeny was scored using the Imaging-PAM Maxi. Bulked segregant pools for *spa1-1* and *cul4-1* were prepared by combining the progeny from each tetrad into 2 separate pools (1 with all high-NPQ progeny and 1 with all low-NPQ progeny) for genomic DNA preparation and whole-genome sequencing. The progeny originated from 7 complete tetrads for both *spa1-1* and *cul4-1*.

The library preparation and sequencing (Illumina HiSeq4000) of the *spa1-1* and *cul4-1* bulked segregant pools was performed at the Vincent J. Coates Genomics Sequencing Laboratory at University of California, (UC), Berkeley. Sequencing reads were filtered and trimmed using Trimmomatic (51), cutadapt (52), and Super-Deduper (53). Overlapping paired reads were merged using Flash (54). Cleaned sequence data (paired, merged, and orphan reads) from each individual sample were then aligned to the reference genome (Chlamydomonas_reinhardtii_v5.5) using Novoalign (Novocraft Technologies). Only reads that mapped uniquely to the reference were kept. After alignment, we used Picard (http://broadinstitute.github.io/picard/) to add read groups and GATK (55) to perform realignment. We used GATK HaplotypeCaller to determine SNP and short indel variants from each individual with the aim of retaining all potential variants. For the resequencing of *npq4*, *spa1-1*, *spa1-2*, and *cul4-1*, the same sequencing and bioinformatic pipeline tools were used. The final coverage for the resequenced samples and the bulked segregant pools (*spa1-1* high NPQ progeny, *spa1-1* low NPQ progeny, *cul4-1* high NPQ progeny, *cul4-1* low NPQ progeny) was ~100×. For *spa1-1*, 3 filtered variants in Cre13.g591050, Cre13.g591150, and

Cre13.g602700 (*SPA1*) had an alternate allele frequency of 100% in the high NPQ pool vs. 0% in the low NPQ pool, each with a minimum coverage of 149× for these 3 variants (*SI Appendix*, Table S1). For *cul4-1*, the maximum alternative allele frequency among the filtered variants was 99.6% in the high NPQ pool vs. 0.01% in the low NPQ pool, and this variant was located in Cre12.g516500 (*CUL4*) with a minimum coverage of 197× (*SI Appendix*, Table S2). The mutation in *spa1-2* was identified by resequencing; Cre13.g602700 (*SPA1*) was the only gene that contained mutations in both *spa1-1* and *spa1-2*.

Complementation of *npq4 spa1-1* and *crco spa1-1*. To complement *npq4 spa1-1*, an 8.5-kb fragment was amplified by PCR with KOD hot start DNA polymerase (Millipore) and primers gSPA1-F and gSPA1-R (*SI Appendix*, Table S3) from a BAC clone (3M23) containing *C. reinhardtii* genomic DNA of this region. The 8.5-kb fragment contains 981 bp upstream of the start codon, the *SPA1* gene, and the endogenous 3′-UTR. The PCR product was cloned using the Zero Blunt TOPO PCR Cloning kit (Thermo Fisher Scientific) and confirmed by sequencing. The *npq4 spa1-1* strain was cotransformed by electroporation with the *SPA1* plasmid and linearized pSL18 (56) that confers paromomycin resistance. Out of 150 transformants screened, 11 showed low NPQ like that of *npq4*. As expected, none of the 350 transformants obtained with only the pSL18 vector showed a low level of NPQ.

For complementation of *crco spa1-1* with *CrCO*, a 1.8-kb fragment containing the *CrCO* coding region was amplified by PCR with Platinum Pfx DNA polymerase (Thermo Fisher Scientific) and primers COcds-F and COcds-R (*SI Appendix*, Table S3) from WT genomic DNA. The resulting PCR product was cloned into pSL18 using In-Fusion (Clontech) for expression under control of the *PSAD* promoter. Sequencing of this construct revealed that a 1-bp insertion had occurred just prior to the FLAG sequence and as a consequence, the FLAG tag was not present in the translated protein. The *crco spa1-1* strain was cotransformed with the *CrCO* plasmid and pBC1-Hyg plasmid containing the *APH7* gene that confers resistance to hygromycin B (57). Out of the 42 transformants screened, 2 showed high NPQ like that of *spa1-1*. None of the 258 transformants obtained with only the pBC1-Hyg vector showed high NPQ.

Protein Extraction and Immunoblot Analysis. Protein was extracted and prepared for SDS/PAGE as described (58) with minor modifications. Protein was quantified by using the BCA1 kit (Sigma-Aldrich) after extraction with methanol and chloroform (59). Protein samples were adjusted to 10 μg of protein per lane for all blots except for that of PSBS, for which 30 μg of protein was loaded per lane for better detection. Proteins were separated by SDS/PAGE on Novex 10 to 20% Tris-glycine gels (Thermo Fisher Scientific). Proteins were transferred to 0.4-μm PVDF membranes (Amersham) for immunoblotting. Antibodies against LHCSR1, LHCSR3, and ATP synthase beta-subunit

(ATPB) (Agrisera) were used at 1:3,000 dilution in 1% milk. The PSBS antibody (17) was a kind gift from Peter Jahns, University of Düsseldorf, Düsseldorf, Germany, and used at 1:1,000 dilution in 1% milk in TBS with 0.1% Tween. The blots were developed using enhanced chemiluminescence substrate SuperSignal West Femto Maximum Sensitivity Substrate (Thermo Fisher Scientific) and imaged and analyzed using the ChemiDoc MP Imaging System and accompanying software Image Lab 5.2.1 (Bio-Rad).

For immunoblots shown in the supplemental figures, protein was extracted by 2 rounds of freeze-thaw of cells resuspended in 10 mM Na_2HPO_4 (pH7.0) buffer, after which chlorophyll was quantified by measuring A_{652}. Protein was solubilized for SDS/PAGE with denaturing buffer (60). Protein equivalent to 1.5 μg chlorophyll was loaded to each lane. Antibody against LHCSR (61) detecting both LHCSR1 and LHCSR3 was used at 1:3,000 dilution in 1% milk in TBS with 0.1% Tween.

Gene Expression Analysis Using Real-Time qPCR. RNA extraction, cDNA synthesis, and qPCR were performed as previously described (62). All primer pairs (*SI Appendix*, Table S3) were confirmed as having 90 to 105% amplification efficiency and linear amplification within their dynamic range in experimental samples using serial dilutions of cDNA prior to the experiments. Relative transcript levels were calculated by ΔΔCt method (63) using CβLP as the internal reference. Primers were designed using Primer3 (64) against the 3′-UTR of each gene to avoid binding to off-target paralogous genes. A single peak in melt curve analysis with a unique melting temperature was observed for each amplicon, verifying that off-target amplification of paralogous genes was negligible.

Motif Analysis. The position-specific scoring matrix for the CO-like binding site upstream of the *C. reinhardtii* qE genes was identified de novo by performing Multiple Em for Motif Elicitation (MEME) (32). To increase the number of sequences submitted to MEME, orthologous promoter sequences from *Volvox carteri* were included.

1. P. Müller, X.-P. Li, K. K. Niyogi, Non-photochemical quenching. A response to excess light energy. *Plant Physiol.* **125**, 1558–1566 (2001).
2. A. V. Ruban, Non-photochemical chlorophyll fluorescence quenching: Mechanism and effectiveness in protection against photodamage. *Plant Physiol.* **170**, 1903–1916 (2016).
3. N. R. Baker, Chlorophyll fluorescence: A probe of photosynthesis in vivo. *Annu. Rev. Plant Biol.* **59**, 89–113 (2008).
4. P. Horton, A. V. Ruban, R. G. Walters, Regulation of light harvesting in green plants. *Annu. Rev. Plant Physiol. Plant Mol. Biol.* **47**, 655–684 (1996).
5. J.-M. Briantais, C. Vernotte, M. Picaud, G. H. Krause, A quantitative study of the slow decline of chlorophyll *a* fluorescence in isolated chloroplasts. *Biochim. Biophys. Acta* **548**, 128–138 (1979).
6. G. Peers et al., An ancient light-harvesting protein is critical for the regulation of algal photosynthesis. *Nature* **462**, 518–521 (2009).
7. G. Bonente et al., Analysis of LhcSR3, a protein essential for feedback de-excitation in the green alga *Chlamydomonas reinhardtii*. *PLoS Biol.* **9**, e1000577 (2011).
8. N. Liguori, L. M. Roy, M. Opacic, G. Durand, R. Croce, Regulation of light harvesting in the green alga *Chlamydomonas reinhardtii*: The C-terminus of LHCSR is the knob of a dimmer switch. *J. Am. Chem. Soc.* **135**, 18339–18342 (2013).
9. M. Ballottari et al., Identification of pH-sensing sites in the light harvesting complex stress-related 3 protein essential for triggering non-photochemical quenching in *Chlamydomonas reinhardtii*. *J. Biol. Chem.* **291**, 7334–7346 (2016).
10. X.-P. Li et al., Regulation of photosynthetic light harvesting involves intrathylakoid lumen pH sensing by the PsbS protein. *J. Biol. Chem.* **279**, 22866–22874 (2004).
11. N. Betterle et al., Light-induced dissociation of an antenna hetero-oligomer is needed for non-photochemical quenching induction. *J. Biol. Chem.* **284**, 15255–15266 (2009).
12. M. P. Johnson et al., Photoprotective energy dissipation involves the reorganization of photosystem II light-harvesting complexes in the grana membranes of spinach chloroplasts. *Plant Cell* **23**, 1468–1479 (2011).
13. L. Wilk, M. Grunwald, P. N. Liao, P. J. Walla, W. Kühlbrandt, Direct interaction of the major light-harvesting complex II and PsbS in nonphotochemical quenching. *Proc. Natl. Acad. Sci. U.S.A.* **110**, 5452–5456 (2013).
14. J. Sacharz, V. Giovagnetti, P. Ungerer, G. Mastroianni, A. V. Ruban, The xanthophyll cycle affects reversible interactions between PsbS and light-harvesting complex II to control non-photochemical quenching. *Nat. Plants* **3**, 16225 (2017).
15. V. Correa-Galvis, G. Poschmann, M. Melzer, K. Stühler, P. Jahns, PsbS interactions involved in the activation of energy dissipation in Arabidopsis. *Nat. Plants* **2**, 15225 (2016).
16. T. Tibiletti, P. Auroy, G. Peltier, S. Caffarri, *Chlamydomonas reinhardtii* PsbS protein Is functional and accumulates rapidly and transiently under high light. *Plant Physiol.* **171**, 2717–2730 (2016).
17. V. Correa-Galvis et al., Photosystem II subunit PsbS is involved in the induction of LHCSR protein-dependent energy dissipation in *Chlamydomonas reinhardtii*. *J. Biol. Chem.* **291**, 17478–17487 (2016).
18. G. Allorent et al., UV-B photoreceptor-mediated protection of the photosynthetic machinery in *Chlamydomonas reinhardtii*. *Proc. Natl. Acad. Sci. U.S.A.* **113**, 14864–14869 (2016).
19. S. S. Merchant et al., The *Chlamydomonas* genome reveals the evolution of key animal and plant functions. *Science* **318**, 245–250 (2007).
20. D. Petroutsos et al., A blue-light photoreceptor mediates the feedback regulation of photosynthesis. *Nature* **537**, 563–566 (2016).
21. K. Tilbrook et al., UV-B perception and acclimation in *Chlamydomonas reinhardtii*. *Plant Cell* **28**, 966–983 (2016).
22. G. Allorent, D. Petroutsos, Photoreceptor-dependent regulation of photoprotection. *Curr. Opin. Plant Biol.* **37**, 102–108 (2017).
23. C. Menon, D. J. Sheerin, A. Hiltbrunner, SPA proteins: SPAnning the gap between visible light and gene expression. *Planta* **244**, 297–312 (2016).
24. U. Hoecker, The activities of the E3 ubiquitin ligase COP1/SPA, a key repressor in light signaling. *Curr. Opin. Plant Biol.* **37**, 63–69 (2017).
25. R. Podolec, R. Ulm, Photoreceptor-mediated regulation of the COP1/SPA E3 ubiquitin ligase. *Curr. Opin. Plant Biol.* **45**, 18–25 (2018).
26. G. Serrano et al., Chlamydomonas CONSTANS and the evolution of plant photoperiodic signaling. *Curr. Biol.* **19**, 359–368 (2009).
27. K. K. Niyogi, O. Björkman, A. R. Grossman, Chlamydomonas xanthophyll cycle mutants identified by video imaging of chlorophyll fluorescence quenching. *Plant Cell* **9**, 1369–1380 (1997).
28. H. Chen et al., *Arabidopsis* CULLIN4-damaged DNA binding protein 1 interacts with CONSTITUTIVELY PHOTOMORPHOGENIC1-SUPPRESSOR OF PHYA complexes to regulate photomorphogenesis and flowering time. *Plant Cell* **22**, 108–123 (2010).

PLANT BIOLOGY

29. D. Zhu *et al*., Biochemical characterization of *Arabidopsis* complexes containing CONSTITUTIVELY PHOTOMORPHOGENIC1 and SUPPRESSOR OF PHYA proteins in light control of plant development. *Plant Cell* **20**, 2307–2323 (2008).

30. X. Holtkotte *et al*., Mutations in the N-terminal kinase-like domain of the repressor of photomorphogenesis SPA1 severely impair SPA1 function but not light responsiveness in Arabidopsis. *Plant J.* **88**, 205–218 (2016).

31. S. Chen *et al*., The functional divergence between SPA1 and SPA2 in Arabidopsis photomorphogenesis maps primarily to the respective N-terminal kinase-like domain. *BMC Plant Biol.* **16**, 165 (2016).

32. T. L. Bailey *et al*., MEME SUITE: Tools for motif discovery and searching. *Nucleic Acids Res.* **37**, W202–W208 (2009).

33. N. Gnesutta *et al*., CONSTANS imparts DNA sequence specificity to the histone fold NF-YB/NF-YC dimer. *Plant Cell* **29**, 1516–1532 (2017).

34. S. Laubinger *et al*., *Arabidopsis* SPA proteins regulate photoperiodic flowering and interact with the floral inducer CONSTANS to regulate its stability. *Development* **133**, 3213–3222 (2006).

35. L.-J. Liu *et al*., COP1-mediated ubiquitination of CONSTANS is implicated in cryptochrome regulation of flowering in *Arabidopsis*. *Plant Cell* **20**, 292–306 (2008).

36. S. Jang *et al*., *Arabidopsis* COP1 shapes the temporal pattern of CO accumulation conferring a photoperiodic flowering response. *EMBO J.* **27**, 1277–1288 (2008).

37. R. M. Dent *et al*., Large-scale insertional mutagenesis of *Chlamydomonas* supports phylogenomic functional prediction of photosynthetic genes and analysis of classical acetate-requiring mutants. *Plant J.* **82**, 337–351 (2015).

38. Y. Aihara, K. Fujimura-Kamada, T. Yamasaki, J. Minagawa, Algal photoprotection is regulated by the E3 ligase CUL4-DDB1^{DET1}. *Nat. Plants* **5**, 34–40 (2019).

39. O. S. Lau, X. W. Deng, The photomorphogenic repressors COP1 and DET1: 20 years later. *Trends Plant Sci.* **17**, 584–593 (2012).

40. D. J. Sheerin *et al*., Light-activated phytochrome A and B interact with members of the SPA family to promote photomorphogenesis in Arabidopsis by reorganizing the COP1/SPA complex. *Plant Cell* **27**, 189–201 (2015).

41. X.-D. Lu *et al*., Red-light-dependent interaction of phyB with SPA1 promotes COP1-SPA1 dissociation and photomorphogenic development in *Arabidopsis*. *Mol. Plant* **8**, 467–478 (2015).

42. X. Huang *et al*., Conversion from CUL4-based COP1-SPA E3 apparatus to UVR8-COP1-SPA complexes underlies a distinct biochemical function of COP1 under UV-B. *Proc. Natl. Acad. Sci. U.S.A.* **110**, 16669–16674 (2013).

43. A. Oravecz *et al*., CONSTITUTIVELY PHOTOMORPHOGENIC1 is required for the UV-B response in *Arabidopsis*. *Plant Cell* **18**, 1975–1990 (2006).

44. B. Liu, Z. Zuo, H. Liu, X. Liu, C. Lin, *Arabidopsis* cryptochrome 1 interacts with SPA1 to suppress COP1 activity in response to blue light. *Genes Dev.* **25**, 1029–1034 (2011).

45. H.-L. Lian *et al*., Blue-light-dependent interaction of cryptochrome 1 with SPA1 defines a dynamic signaling mechanism. *Genes Dev.* **25**, 1023–1028 (2011).

46. Z. Zuo, H. Liu, B. Liu, X. Liu, C. Lin, Blue light-dependent interaction of CRY2 with SPA1 regulates COP1 activity and floral initiation in Arabidopsis. *Curr. Biol.* **21**, 841–847 (2011).

47. B. Beel *et al*., A flavin binding cryptochrome photoreceptor responds to both blue and red light in *Chlamydomonas reinhardtii*. *Plant Cell* **24**, 2992–3008 (2012).

48. N. Müller *et al*., A plant cryptochrome controls key features of the *Chlamydomonas* circadian clock and its life cycle. *Plant Physiol.* **174**, 185–201 (2017).

49. E. H. Harris, *The Chlamydomonas Sourcebook* (Academic Press, Inc., San Diego, 1989).

50. S. S. McCarthy, M. C. Kobayashi, K. K. Niyogi, White mutants of *Chlamydomonas reinhardtii* are defective in phytoene synthase. *Genetics* **168**, 1249–1257 (2004).

51. A. M. Bolger, M. Lohse, B. Usadel, Trimmomatic: A flexible trimmer for Illumina sequence data. *Bioinformatics* **30**, 2114–2120 (2014).

52. M. Martin, Cutadapt removes adapter sequences from high-throughput sequencing reads. *EMBnet J.* **17**, 10–12 (2011).

53. K. R. Petersen, D. A. Streett, A. T. Gerritsen, S. S. Hunter, M. L. Settles, "Super deduper, fast PCR duplicate detection in fastq files" in *Proceedings of the 6th ACM Conference on Bioinformatics, Computational Biology and Health Informatics* (Association for Computing Machinery, New York, 2015), pp. 491–492.

54. T. Magoč, S. L. Salzberg, FLASH: Fast length adjustment of short reads to improve genome assemblies. *Bioinformatics* **27**, 2957–2963 (2011).

55. A. McKenna *et al*., The genome analysis toolkit: A MapReduce framework for analyzing next-generation DNA sequencing data. *Genome Res.* **20**, 1297–1303 (2010).

56. N. Depège, S. Bellafiore, J.-D. Rochaix, Role of chloroplast protein kinase Stt7 in LHCII phosphorylation and state transition in *Chlamydomonas*. *Science* **299**, 1572–1575 (2003).

57. P. Berthold, R. Schmitt, W. Mages, An engineered *Streptomyces hygroscopicus aph 7"* gene mediates dominant resistance against hygromycin B in *Chlamydomonas reinhardtii*. *Protist* **153**, 401–412 (2002).

58. R. H. Calderon *et al*., A conserved rubredoxin is necessary for photosystem II accumulation in diverse oxygenic photoautotrophs. *J. Biol. Chem.* **288**, 26688–26696 (2013).

59. D. Wessel, U.-I. Flügge, A method for the quantitative recovery of protein in dilute solution in the presence of detergents and lipids. *Anal. Biochem.* **138**, 141–143 (1984).

60. U. K. Laemmli, Cleavage of structural proteins during the assembly of the head of bacteriophage T4. *Nature* **227**, 680–685 (1970).

61. C. Richard, H. Ouellet, M. Guertin, Characterization of the LI818 polypeptide from the green unicellular alga *Chlamydomonas reinhardtii*. *Plant Mol. Biol.* **42**, 303–316 (2000).

62. S. Wakao *et al*., Phosphoprotein SAK1 is a regulator of acclimation to singlet oxygen in *Chlamydomonas reinhardtii*. *eLife* **3**, e02286 (2014).

63. K. J. Livak, T. D. Schmittgen, Analysis of relative gene expression data using real-time quantitative PCR and the 2(-Δ Δ C(T)) method. *Methods* **25**, 402–408 (2001).

64. A. Untergasser *et al*., Primer3–New capabilities and interfaces. *Nucleic Acids Res.* **40**, e115 (2012).